ELSEVIER

Journal of Nuclear Materials 258–263 (1998) 1997–2001

journal of nuclear materials

Microstructural evolution of welded austenitic stainless steel irradiated in HFIR target experiments [1]

T. Sawai *, K. Shiba, A. Hishinuma

Japan Atomic Energy Research Institute, Tokai-mura, Ibaraki-ken 319-11, Japan

Abstract

Microstructural evolution of welded austenitic stainless steel irradiated with mixed-spectrum neutrons was examined by transmission electron microscopy (TEM). TEM disks were obtained from electron-beam (EB) welded plates of JPCA, which is a Ti-midified austenitic stainless steel. Specimens were irradiated in HFIR up to 17 dpa at 670 and 770 K, and the estimated helium concentration was around 1100 appm. Cavities formed at 670 K irradiation were very small (<8 nm) bubbles, and swelling was thus small. At 770 K irradiation, cellular microstructure was observed in weld metal specimens and the cavity microstructure was heterogeneous. Large cavities up to 30 nm were observed in the cell center region while cavities at the cell boundary remained small bubbles. Ti segregation during solidification of weld metal is reflected on the cavity microstructure. EB welding with Ti foil insertion to modify the weld metal had little effect on preventing the degradation of swelling resistance.

1. Introduction

Intensive efforts have been devoted to clarify the radiation response of austenitic stainless steels, which are near-term candidates for fusion structural applications. One of the problems with this type of alloy is void swelling, and alloy development has often involved the addition of minor elements to suppress it. Titanium addition to JPCA, for example, was very successful to reduce the void swelling in neutron irradiation [1,2].

The core components of fusion reactors will be assembled and/or constructed using welding. Welding would also be used for their repair. It is, however, reported that welding affects the swelling behavior of austenitic stainless steels [3,4]. Electron irradiation experiments in a high voltage electron microscope (HVEM) have shown a significant degradation in swelling resistance at the weld metal of electron-beam (EB) welded JPCA [3]. Segregation of major and minor elements during solidification is inevitable in the weld metal, and this produces a characteristic cellular structure. Microstructural analysis and microchemical analysis suggested that the depletion of titanium in the cell center region caused marked degradation in swelling resistance and heterogeneous microstructural evolution in the electron-irradiated weld metal.

It is well recognized that transmutation helium plays an important role in the microstructural evolution in the fusion environment. It has been also reported that the swelling behavior of Ti-modified steels irradiated in an HVEM is highly affected by the pre-injected helium [5]. The purpose of present work is to investigate the microstructural evolution of JPCA weld metal irradiated by mixed spectrum neutrons in the High Flux Isotope Reactor (HFIR), where thermal neutrons produce transmutation helium along with the displacement damage due to fast neutrons.

2. Experimental

Plates of JPCA were EB welded. The composition of JPCA is given in Table 1. Some plates were welded with titanium foil insertion to modify the weld metal.

* Corresponding author. Tel.: +81 29 282 6551; fax: +81 29 282 5922; e-mail: sawai@realab01.tokai.jaeri.go.jp

[1] Research sponsored by Japan Atomic Energy Research Institute and the Office of Fusion Energy, US Department of Energy, under contract DE-AC05-84OR21400 with Lochheed Martin Energy Systems.

0022-3115/98/$19.00
PII: S0022-3115(98)00076-2

Table 1
Chemical analysis of JPCA base metal and its weld metals

	Base metal	Standard EB weld	Ti foil insertion EB weld
C	0.052	0.064	0.057
Si	0.51	0.52	0.53
Mn	1.8	1.5	1.44
P	0.028	0.029	0.028
S	0.005	0.003	<0.005
Cr	14.3	15.1	14.5
Ni	15.5	15.9	15.5
Mo	2.3	2.4	2.4
Ti	0.24	0.26	0.28
N	0.0037	0.0012	0.0038
B	0.0031	0.004	0.0037
O	–	<0.0005	0.0029

Hereafter EB welding methods with and without Ti foil insertion are designated as the standard EB weld and Ti foil insertion EB weld. The conditions of EB welding are shown in Table 2. Weld joints were examined by ultrasonic inspection, radiography, and tensile tests. These conventional tests showed no harmful defects in the fabricated weld. The weld metal had a cellular structure, and the typical cell size was 10 μm. Chemical analysis data of weld metals are also given in Table 1.

Disk specimens, 3 mm in diameter and 0.25 mm thick, obtained from these weld joints were irradiated in the target position of HFIR. The disks were irradiated at 670 K in JP-10 position 6 and at 770 K in JP-11 position 6. According to the dosimetry data [6], the damage level and accumulated helium concentration in JPCA irradiated in these two experiments are estimated to be 17 dpa and 1100 appm, respectively.

Preparation of thin foil from irradiated specimens was carried out with a jet polishing unit set in a glove box. The perforated specimens were examined by an optical microscope to make sure that the thin foil was located in weld metal. TEM observation was performed with a JEM-2000FX with a LaB_6 filament operated at 200 kV. Microstructural data were quantified with the specimen thickness value obtained by counting thickness fringes. Microstructural data of standard EB welds were obtained at 670 and 770 K irradiation, and those of Ti foil insertion welds were obtained at 770 K irradiation.

Table 2
EB weld conditions

	Standard EB weld	Ti foil insertion EB weld
Plate thickness	15 mm	15 mm
Electron beam energy	40 kV	60 kV
Electron beam current	350 mA	300 mA
Welding rate	400 mm/min	500 mm/min
Insertion	None	10 μm Ti foil

3. Experimental results

In the weld metal specimen of a standard EB weld irradiated at 670 K, cellular structure was clearly observed. There was little difference between the cavity microstructure in cell boundary region and that in cell center region. Irradiation induced cavities were smaller than 8 nm, and most of them were smaller than 5 nm. Swelling measured as the cavity volume fraction was 0.3%. Frank loops up to 30 nm and very tiny stacking fault tetrahedra (<2 nm) were also observed. MC precipitates identified by Moire fringes are more frequently observed in the cell boundary region than in the cell center region.

Cellular structure was still clearly observed at 770 K irradiation. Microstructural features in the cell boundary region and in the cell center region in an identical specimen are shown in Fig. 1. Cavities, Frank loops, precipitates and dislocations were observed in a kinematical bright field image slightly under-focused, in a dark field image formed with a stacking fault diffraction streak, and in a weak beam dark field image, respectively. It can be clearly seen that the microstructural evolution is quite different in these regions. Micrographs in Fig. 1 represent typical samples at each region. Microstructure varied gradually between these regions. Cavities in the cell center region included a few larger ones up to 30 nm and many smaller ones, while those in the cell boundary region were smaller than 5 nm. The number density of cavities is much higher in the cell boundary region than in the cell center region. Quantified data on cavity statistics obtained from typical micrographs in both regions are shown in Fig. 2. The cell center region showed higher swelling due to fewer but larger cavities than the cell boundary region. Note that the average cavity size in the cell center region shown in Fig. 2 (b) is dominated by tiny but numerous cavities. The size of Frank loops showed little difference in both regions although their number density was higher in the cell center region than in the region of cell boundary. Quantified Frank loop data are shown in Fig. 3. MC precipitates identified by Moire fringes are more frequently observed in the cell boundary region than in the cell center region.

A weld metal specimen taken from a Ti foil insertion EB weld was examined at 770 K irradiation. Cellular structure and heterogeneous cavity formation were also observed in this specimen. A few larger cavities up to 30 nm and many smaller ones were observed in the cell center in this specimen, while the cell boundary contained only small ones (<5 nm). Quantified microstructural data are also included in Figs. 2 and 3. The

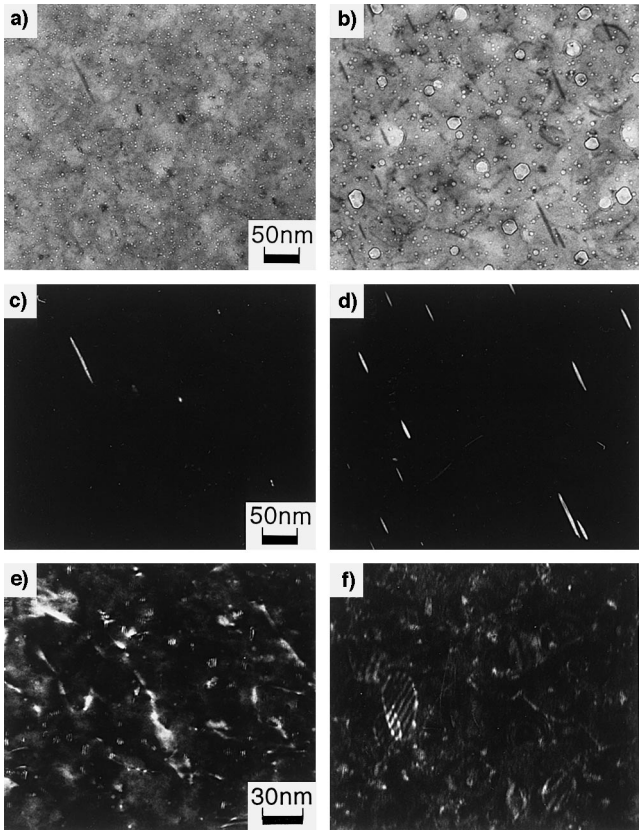

Fig. 1. Microstructural features observed in the weld metal specimen of a standard EB weld irradiated in HFIR at 770 K. (a,c,e) are observed in the cell boundary region and (b,d,f) are in the cell center region. (a) and (b) are cavities, (c) and (d) are Frank loops and (e) and (f) are precipitates and dislocations.

cavity microstructure in weld metal showed little difference from that observed in the standard EB weld specimen. Frank loops and other microstructural features also showed similar heterogeneity as observed in the weld metal specimen of the standard EB weld.

4. Discussion

The preferential thinning in the cell center region shows cellular microstructure in the weld metal [7]. Cellular structure observed in the specimens thinned after irradiation suggests that the segregation in the weld metal has been retained during the irradiation. Microstructural evolution of HFIR-irradiated austenitic stainless steels including JPCA has been studied in the JAERI/DOE collaborative program [1,8–10]. Differences in swelling resistance of various austenitic steels in this irradiation environment become significant at 770 K and higher irradiation temperatures. In the present experiment, initial segregation in the weld metal had little effect on the microstructural evolution at 670 K irradiation. Previous ORR irradiation at 670 K also produced homogeneous cavity microstructure in the JPCA weld metal specimens [2], although differences in swelling resistance of various austenitic steels were shown in the ORR irradiation at 670 K with spectral tailoring [2,11].

The heterogeneity of cavity swelling observed at 770 K irradiation is consistent with that observed in the previous HVEM irradiation of weld metals [3]. The cavity growth rate in the cell center region is much higher than that in the cell boundary region both in HFIR irradiation and HVEM irradiation. The cavity number density is, however, higher in the cell boundary region in HFIR irradiation, while cavity nucleation is also suppressed in the cell boundary region in HVEM irradiation. Enriched Ti at the cell boundary was effective to suppress both nucleation and growth of cavities in HVEM irradiation. These two effects of titanium and how the pre-injected helium affects them are reported [2]. Smaller cavities are unstable due to relatively higher surface energy and lower sink strength to over-saturated vacancies [12]. The surface energy could be reduced by oxygen [13] or nitrogen [14], and trapping of these

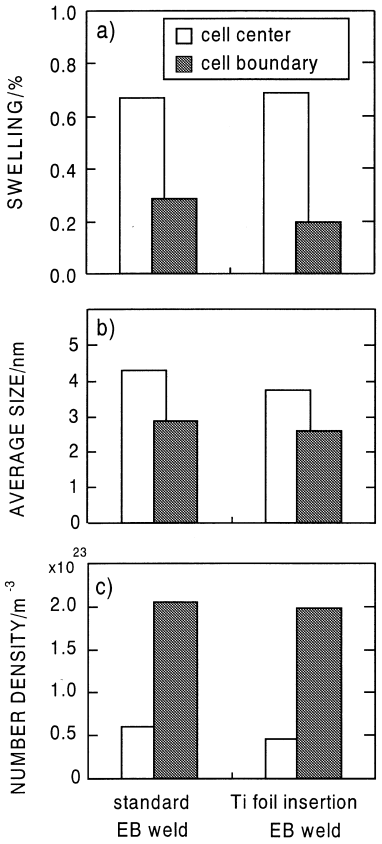

Fig. 2. Quantified cavity data of weld metals irradiated at 770 K.

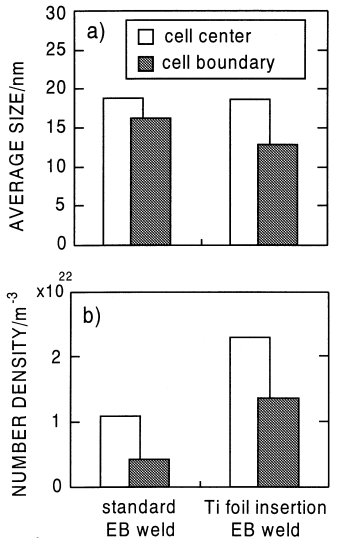

Fig. 3. Quantified Frank loop data of weld metals irradiated at 770 K.

elements by titanium makes nucleation of cavities difficult. Helium, pre-injected or generated by transmutation, is another stabilizer for small cavities. Without sufficient sink strength and vacancy over-saturation, gas pressure of contained helium maintains tiny cavities smaller than the critical size [12]. The heterogeneous cavity microstructure observed in HVEM irradiation [3] thus reflects the effect of titanium to suppress cavity nucleation which would not be effective in a fusion environment. Nevertheless, enhanced swelling in the cell center region due to initial segregation is again demonstrated in the present experiment where transmutation helium is generated during the irradiation.

The cavity microstructure observed in the cell center region irradiated at 770 K shows the typical bi-modal size distribution. Cavities which had once exceeded the critical size had grown rapidly due to their sufficient sink strength, although the quantified cavity size data shown in Fig. 2(b) reflect many small cavities. On the other hand, tiny cavities in the cell boundary seem to be helium bubbles which will grow slowly. The reported microstructure of HFIR-irradiated JPCA at 34 dpa and 770 K includes cavities up to 25 nm and swelling of 0.51% [1]. Present cavity data obtained in the cell center region exceed these values only at 17 dpa. Although the gradual change of the cavity microstructure in weld metal makes it difficult to evaluate the accurate average swelling, the swelling of JPCA weld metal would be larger than that of base metal.

A Ti foil insertion EB weld was employed in the present experiment. It was applied to a Type 316 stainless steel without titanium and suppressed the swelling in the weld metal [15]. In the present experiment, however, Ti foil insertion made little improvement compared with standard EB welds in suppressing swelling in weld metal of JPCA.

5. Summary

Weld metal specimens taken from EB welds of JPCA were irradiated in a HFIR target position to a displacement level of up to 17 dpa. Specimens included those obtained from Ti foil insertion EB welds. TEM observation of specimens irradiated at 670 and 770 K revealed followings;

1. At 670 K irradiation, cavity microstructure was homogeneous in the weld metal, where cellular structure was clearly observed. Cavities were smaller than 8 nm.
2. At 770 K irradiation, enhanced swelling was observed in the cell center region. Larger cavities up to 30 nm were observed in the cell center region while the cell boundary region contained only tiny cavities. The number density of cavities in the cell boundary was higher than that in the cell center region.

3. Compared with the cavity data previously obtained for JPCA base metal, the swelling resistance of JPCA weld metal is degraded.
4. Ti foil insertion in an EB weld had little effect in preventing the degradation of swelling resistance of the weld metal.

References

[1] M.P. Tanaka et al., J. Nucl. Mater. 155–157 (1988) 801.
[2] T. Sawai, P.J. Maziasz, A. Hishinuma, J. Nucl. Mater. 179-181 (1991) 519.
[3] T. Sawai et al., J. Nucl. Mater. 141–143 (1986) 444.
[4] A. Kohyama, Y. Kohno, A. Hishinuma, J. Nucl. Mater. 212–215 (1994) 1579.
[5] T. Sawai et al., J. Nucl. Mater. 212–215 (1994) 453.
[6] L.R. Greenwood, R.T. Ratner, FRM Semiannual Prog. Rep. Dec. 31, 1995, USDOE, Office of Fusion Energy, DOE/ER-0313/19, p. 281.
[7] J.A. Brooks, J.C. Williams, A.W. Thompson, Met. Trans. 14A (1983) 23.
[8] M.P. Tanaka et al., J. Nucl. Mater. 141–143 (1986) 943.
[9] S. Hamada et al., J. Nucl. Mater. 155–157 (1988) 838.
[10] M. Suzuki et al., in: N.H. Packan, R.E. Stoller, A.S. Kumar, Effects of Radiation on Materials: 14th International Symposium, ASTM-STP 1046, vol. 1, ASTM, Philadelphia, 1989, p. 172.
[11] T. Sawai et al., J. Nucl. Mater. 191–194 (1992) 712.
[12] L.K. Mansur, W.A. Coghlan, J. Nucl. Mater. 119 (1983) 1.
[13] S.J. Zinkle et al., Philos. Mag. 55A (1987) 127.
[14] N. Igata et al., J. Nucl. Mater. 212–215 (1994) 341.
[15] T. Sawai et al., J. Nucl. Mater. 155–157 (1988) 861.